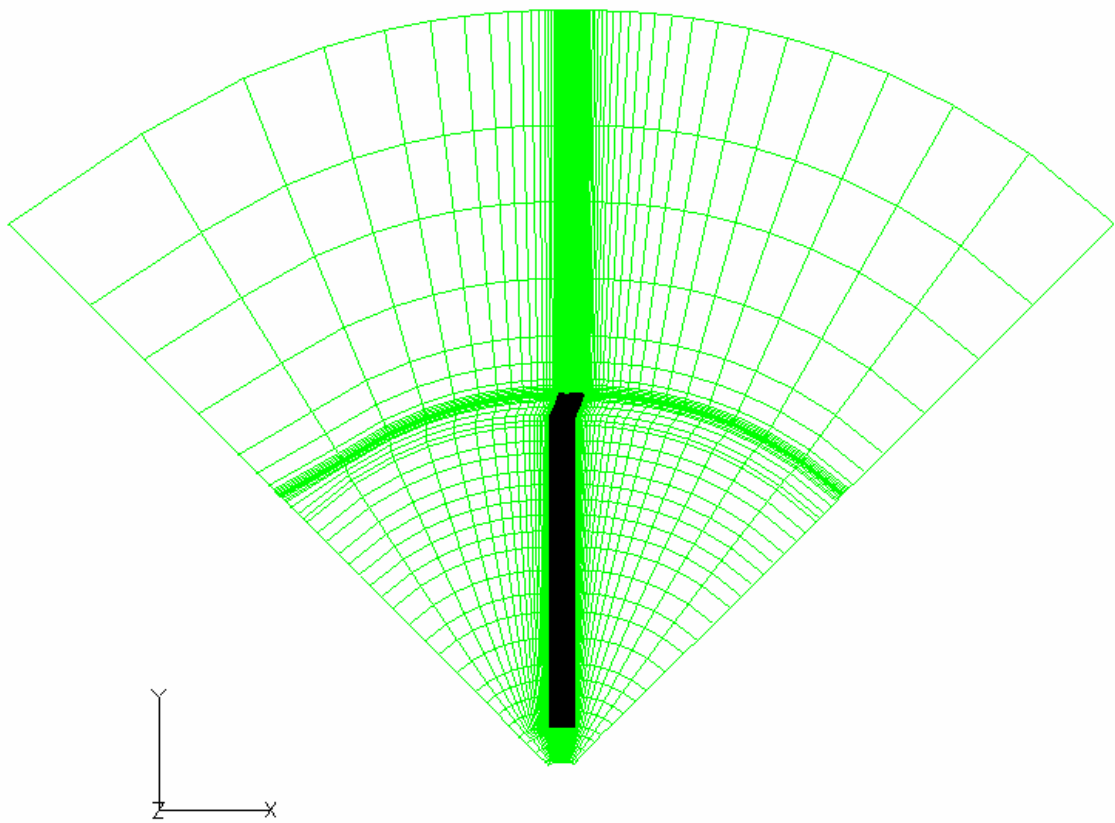
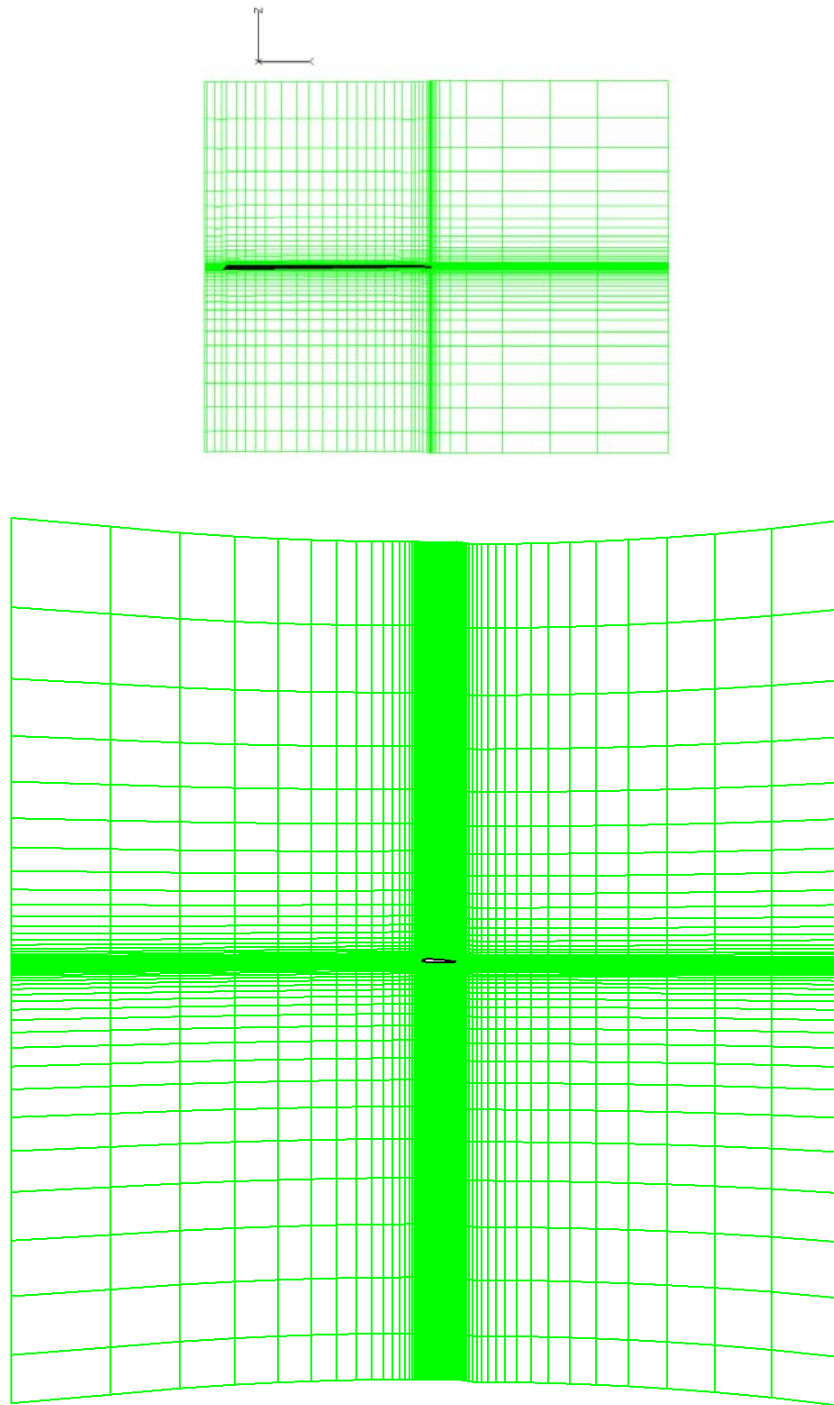


Figure 4.4: Grid Structure for the UH-60A Blade



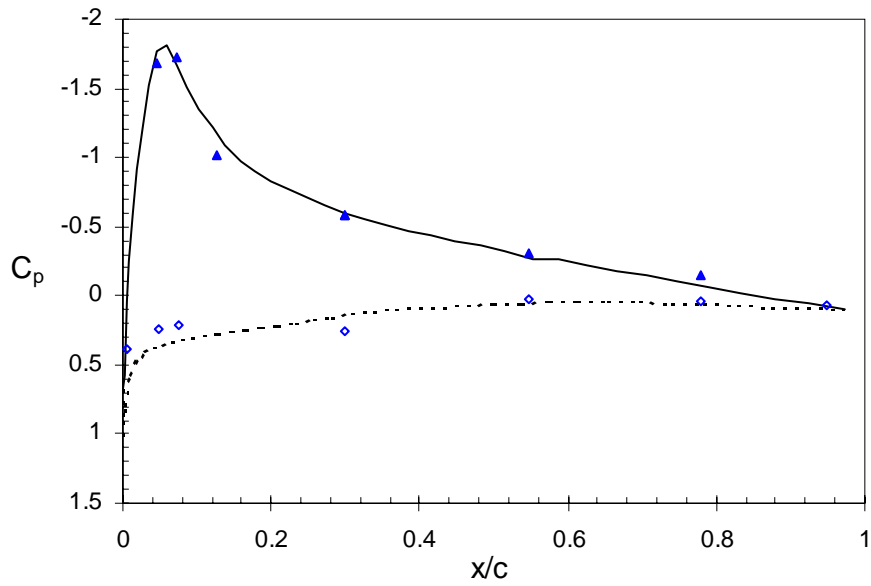
(a) top view

Figure 4.5: Three Views of the Grid around a UH-60A Blade



(b) side view

Figure 4.5: Three Views of the Grid around a UH-60A Blade



(a) $r/R=67.5\%$

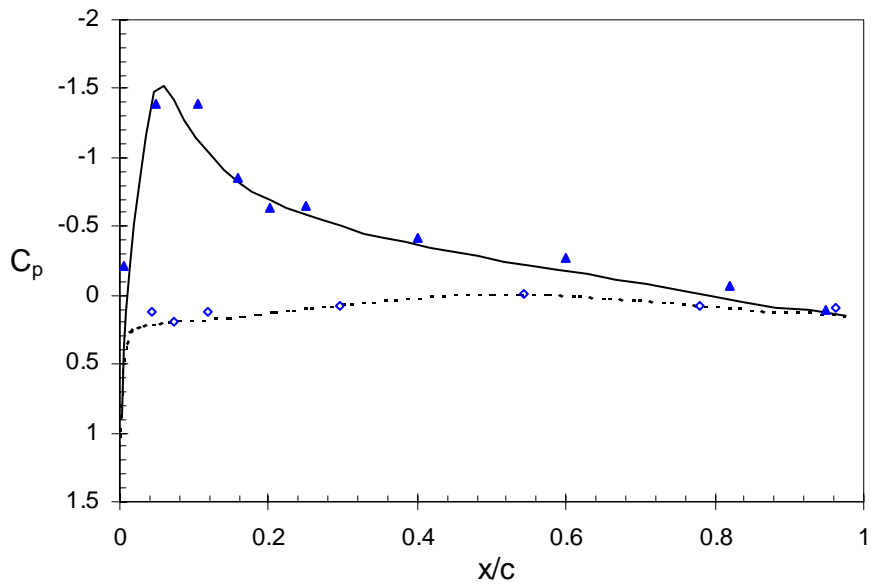
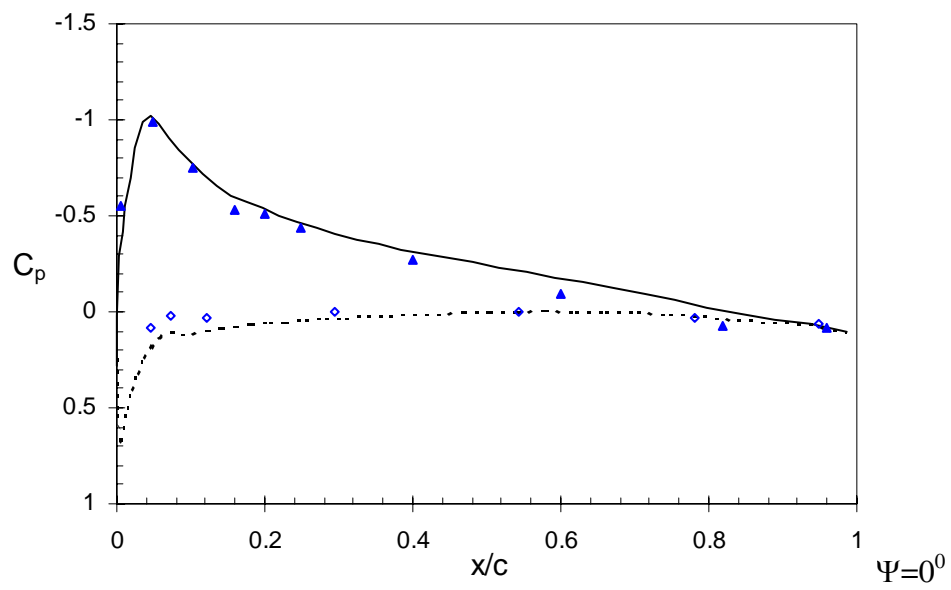
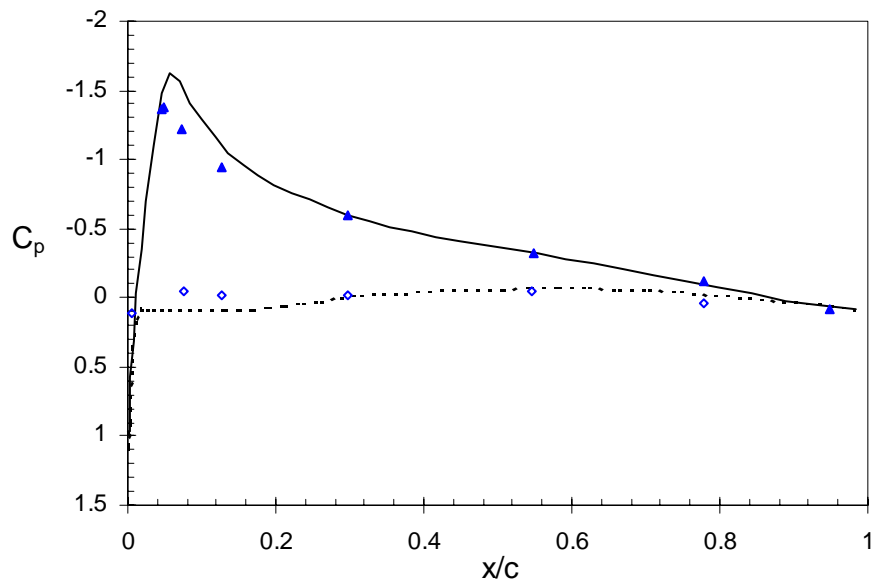
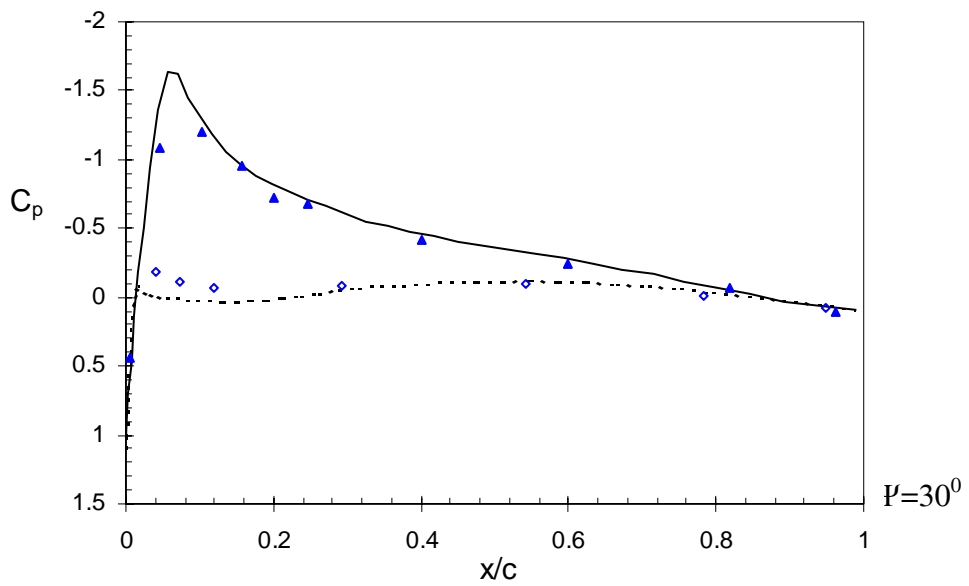


Figure 4.6: Pressure Coefficients for the UH-60A Rotor at $\Psi=0^0$



(a) $r/R=67.5\%$



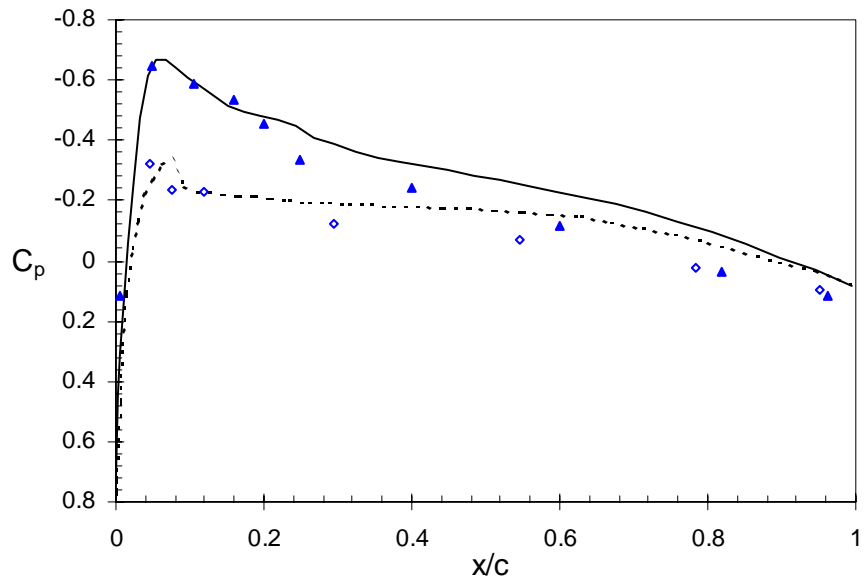
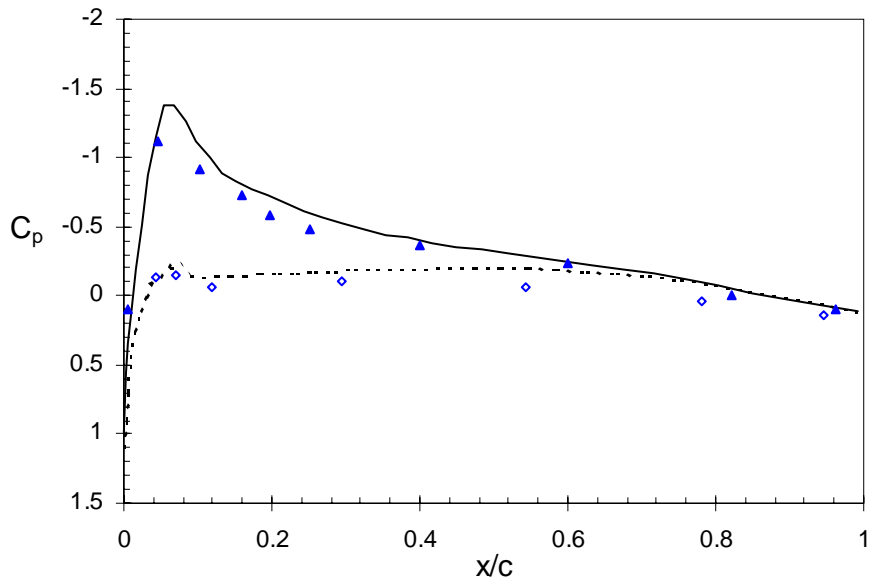
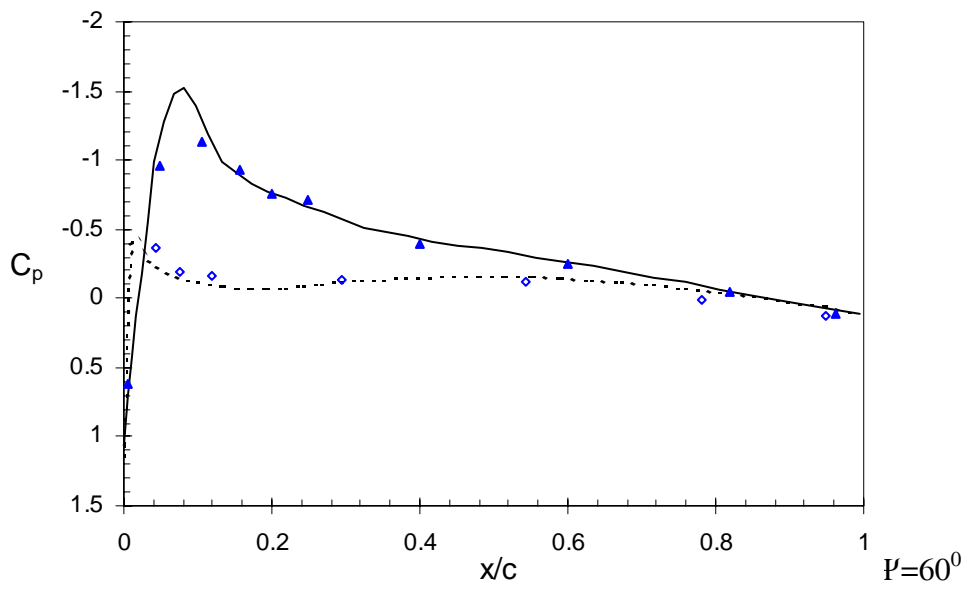
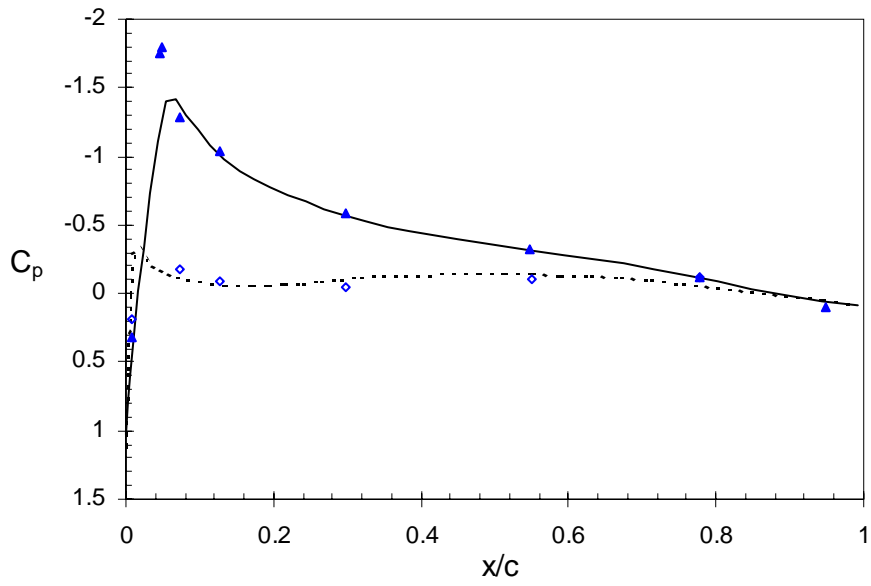
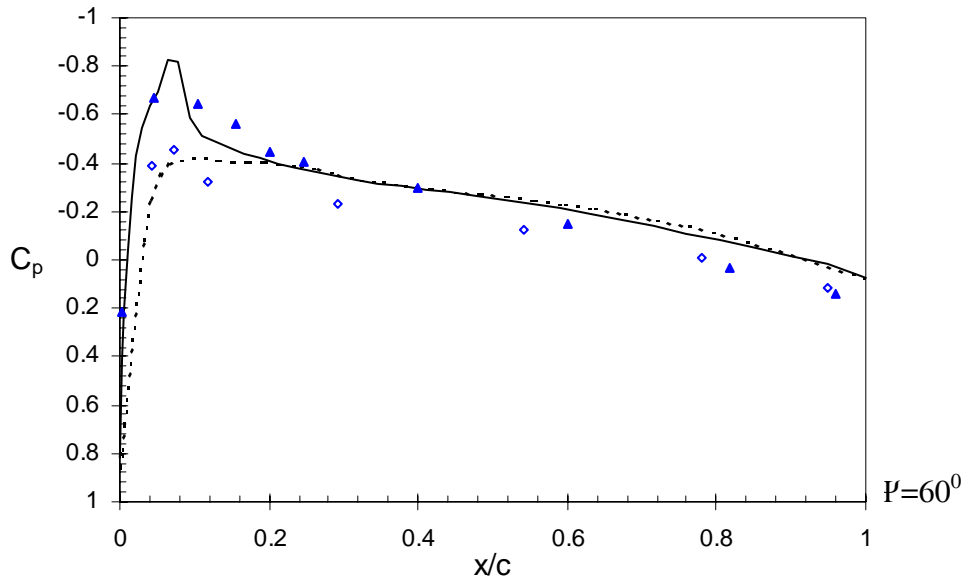
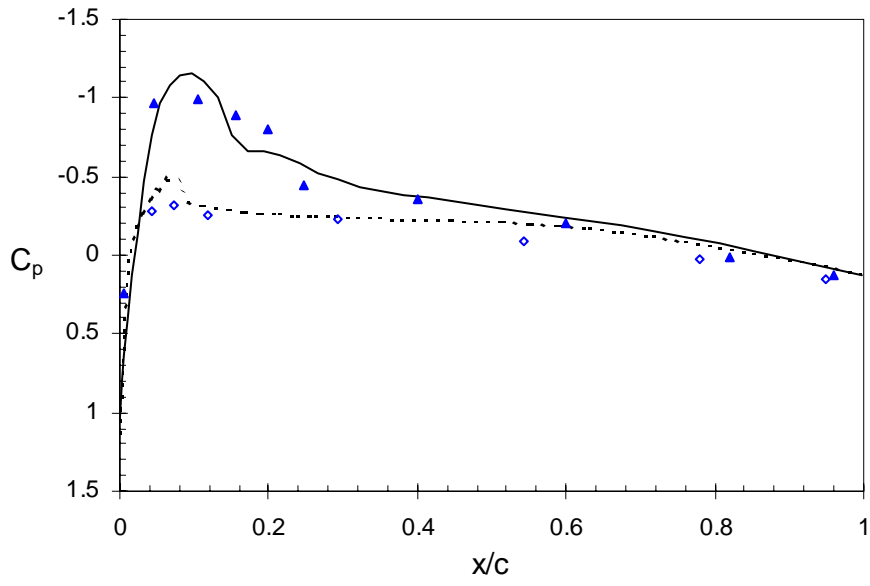
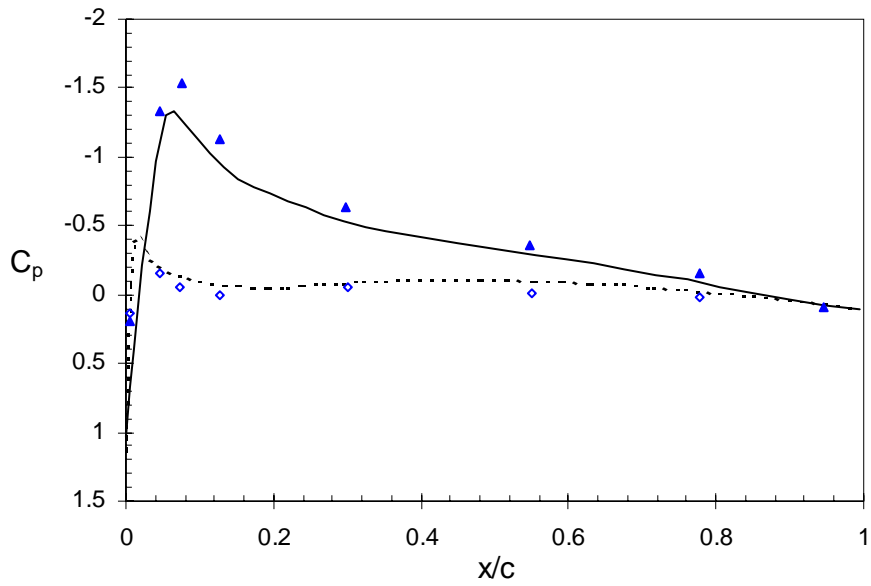


Figure 4.7: Pressure Coefficients for the UH-60A Rotor at $\Psi=30^0$







(a) $r/R=67.5\%$

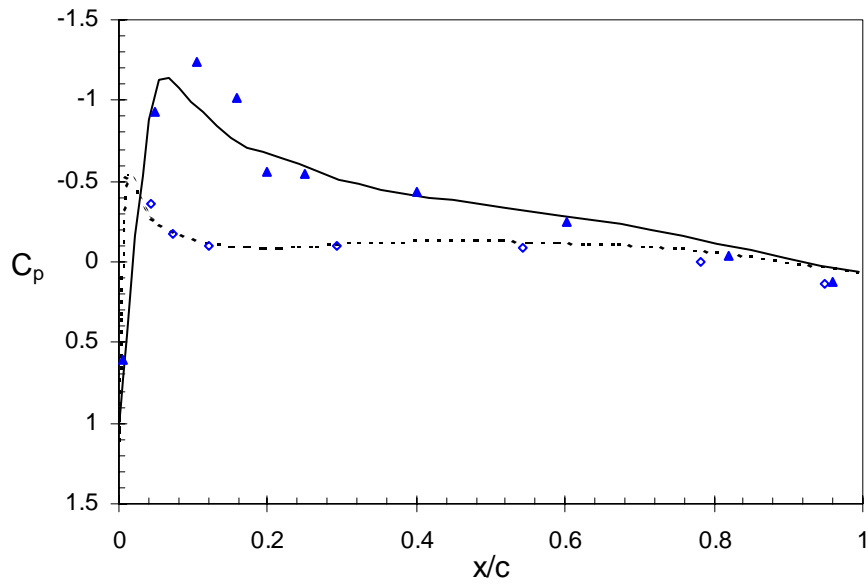
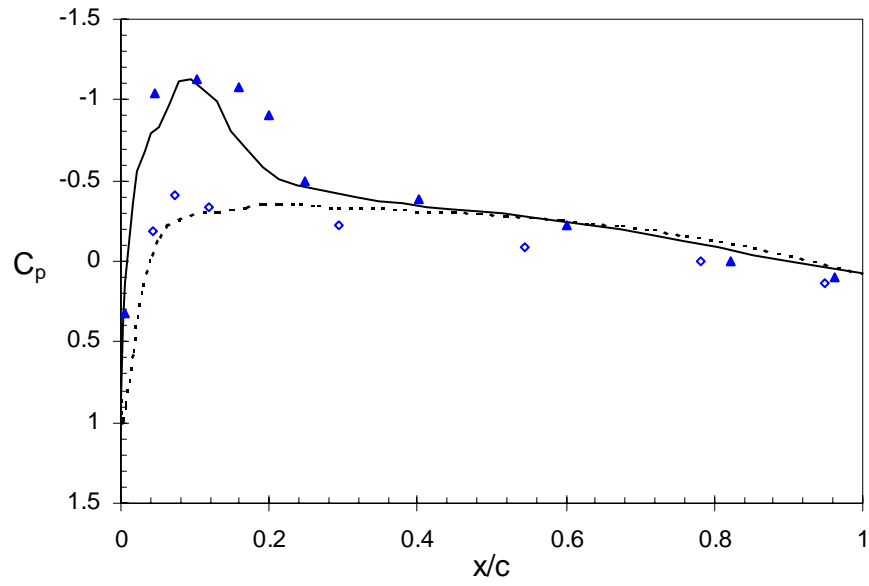


Figure 4.9: Pressure Coefficients for the UH-60A Rotor at $\Psi=90^0$



(c) $r/R=86.5\%$

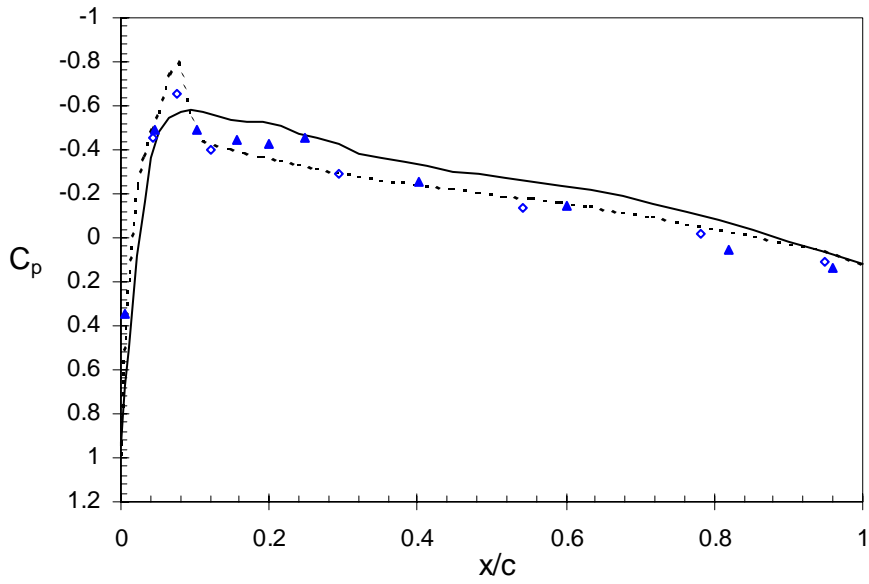
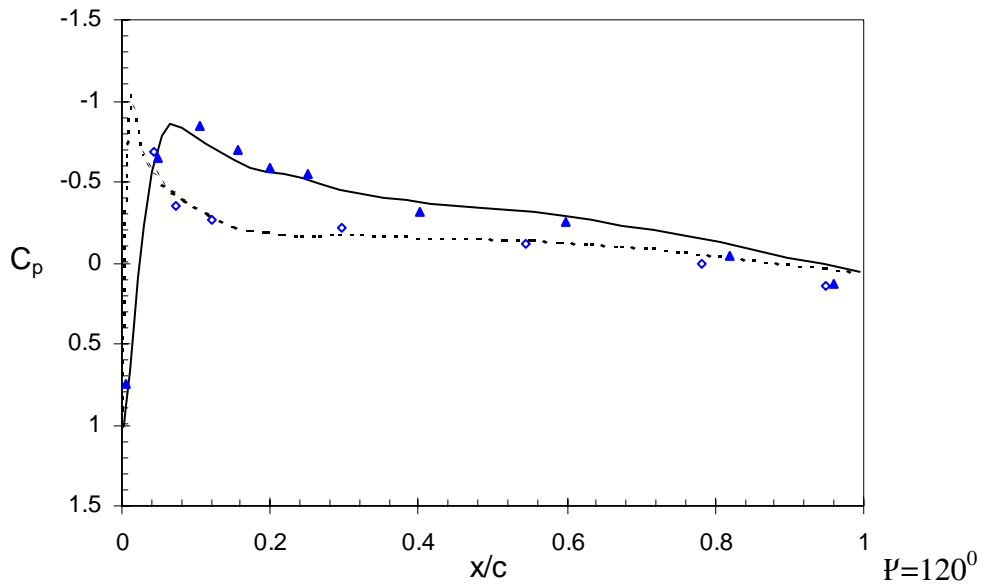
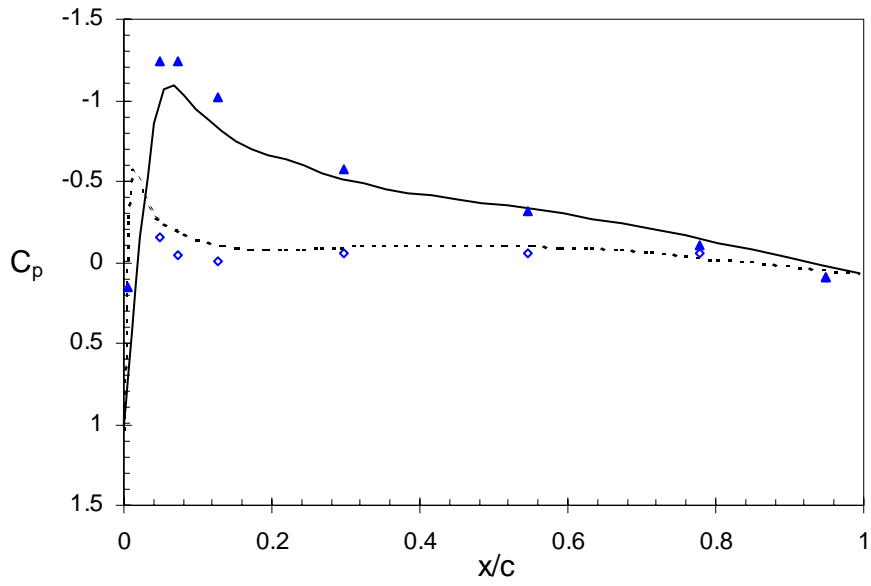
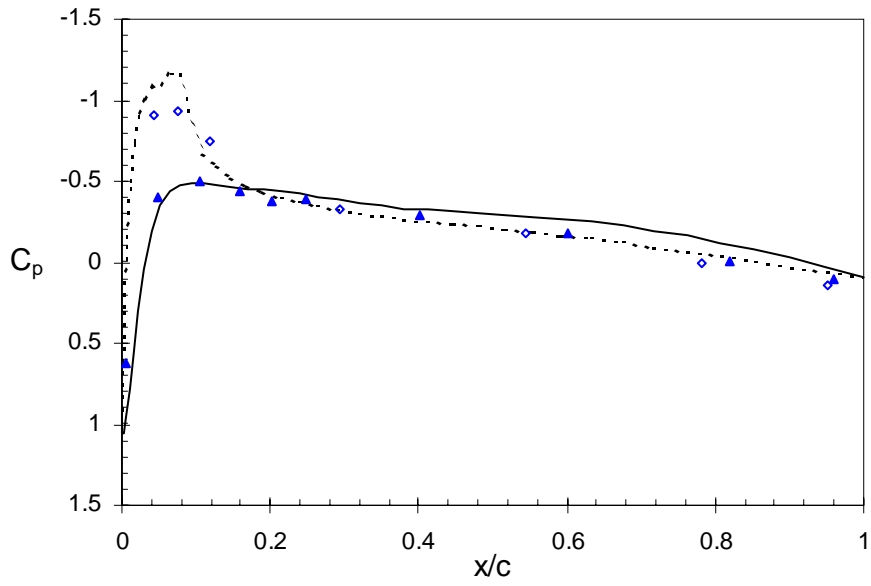


Figure 4.9: Pressure Coefficients for the UH-60A Rotor at $\Psi=90^0$





(c) $r/R=86.5\%$

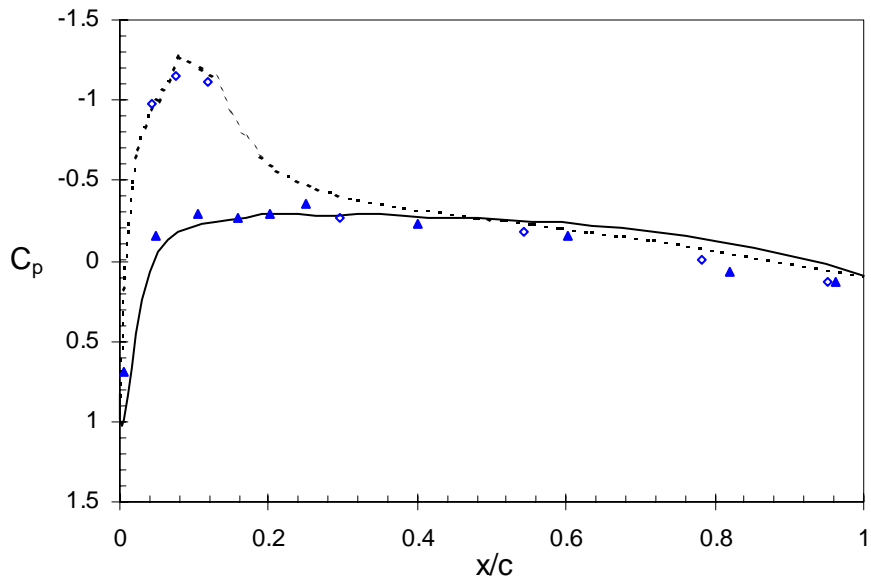
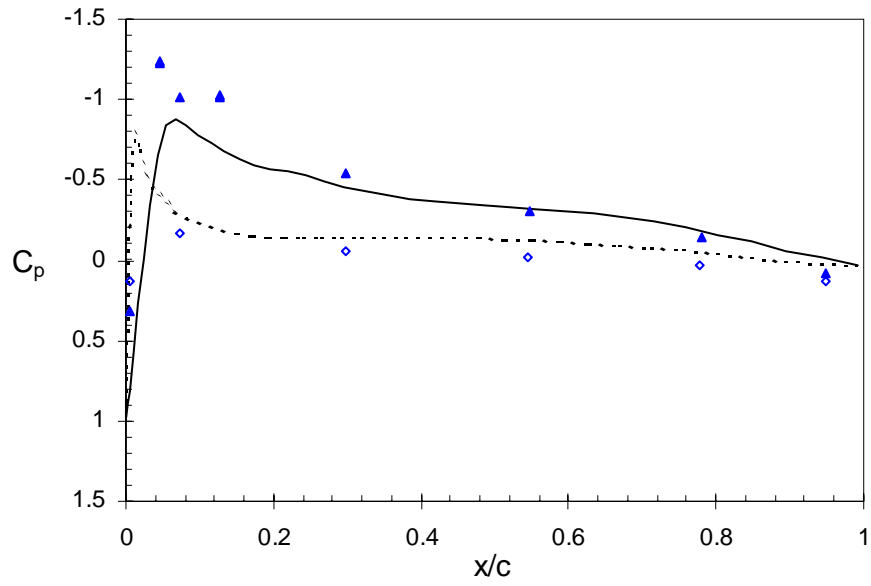


Figure 4.10: Pressure Coefficients for the UH-60A Rotor at $\Psi=120^\circ$



(a) $r/R=67.5\%$

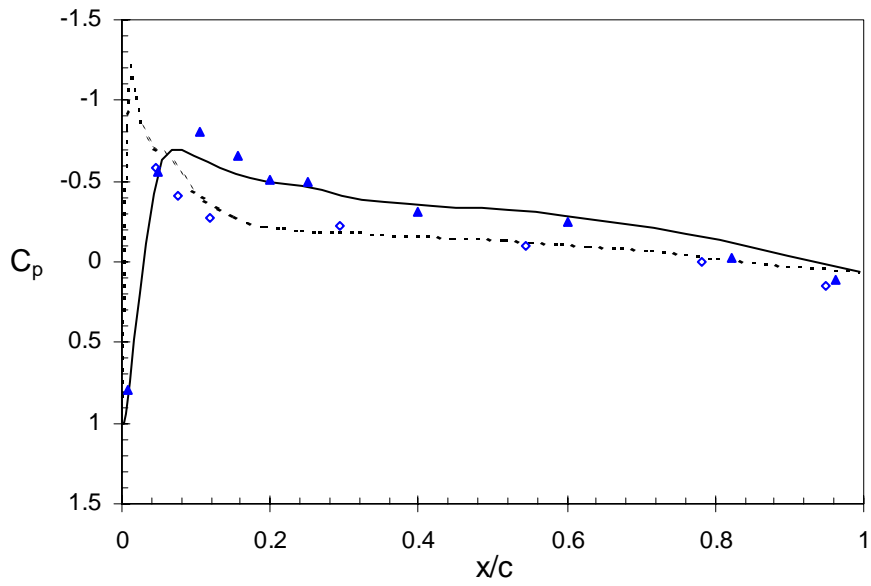
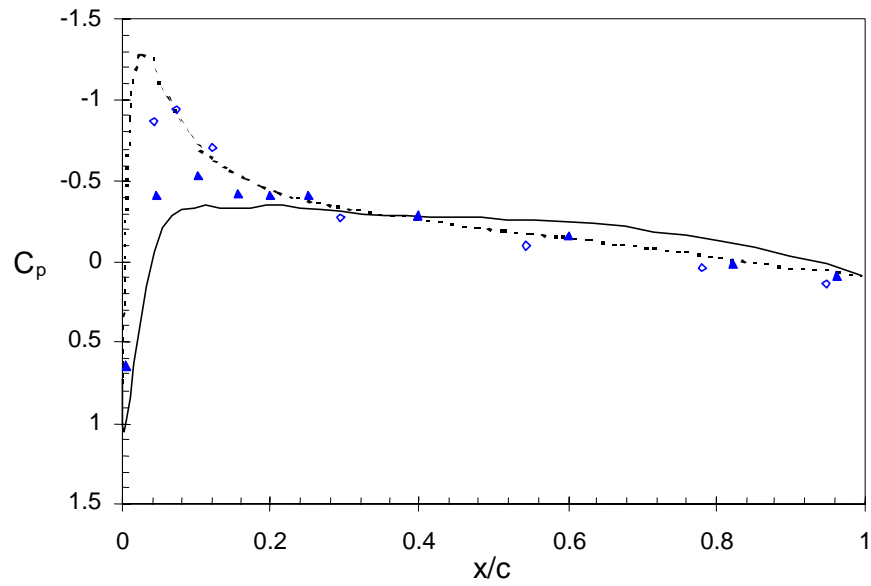


Figure 4.11: Pressure Coefficients for the UH-60A Rotor at $\Psi=150^0$



(c) $r/R=86.5\%$

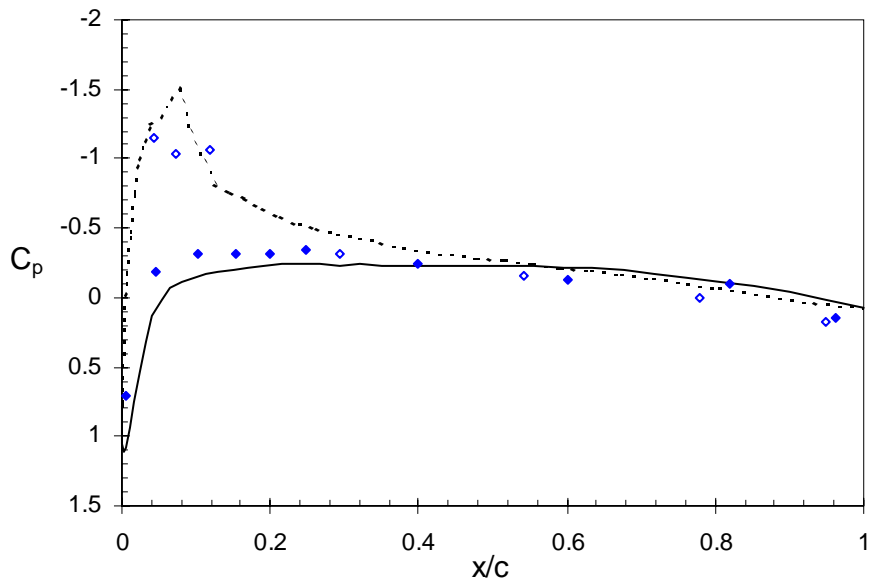
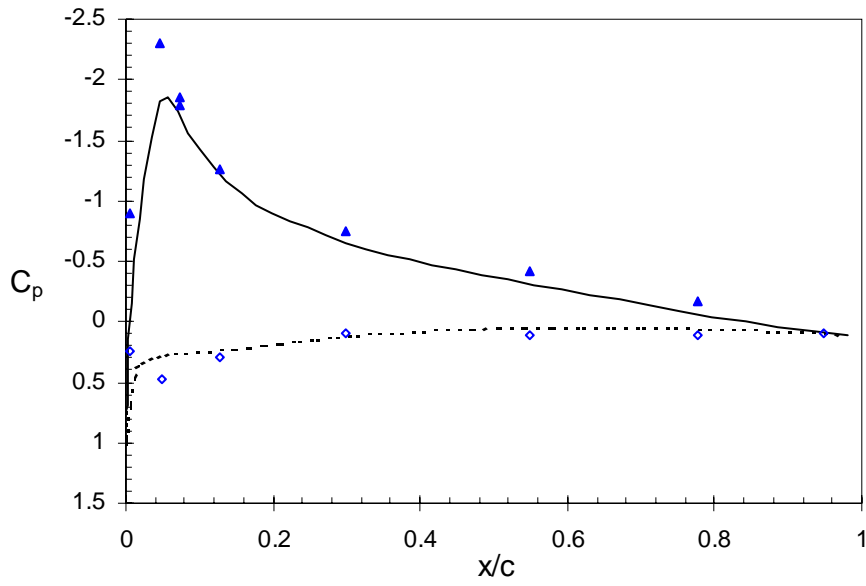


Figure 4.11: Pressure Coefficients for the UH-60A Rotor at $\Psi=150^0$



(a) $r/R=67.5\%$

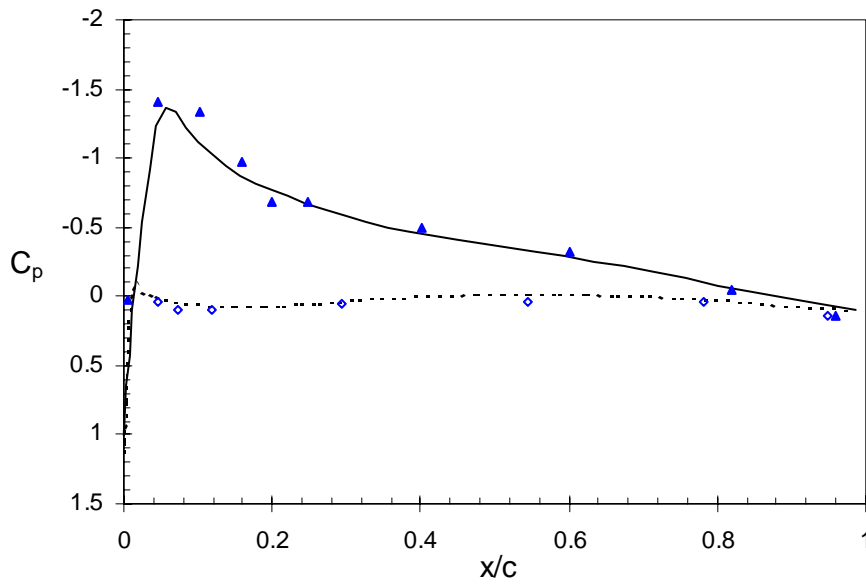
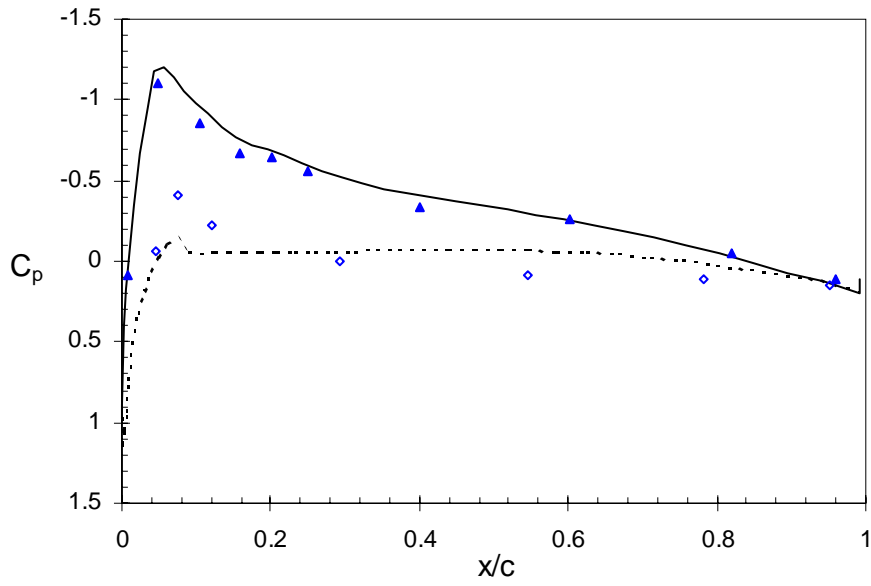


Figure 4.12: Pressure Coefficients for the UH-60A Rotor at $\Psi=180^0$



(c) $r/R=86.5\%$

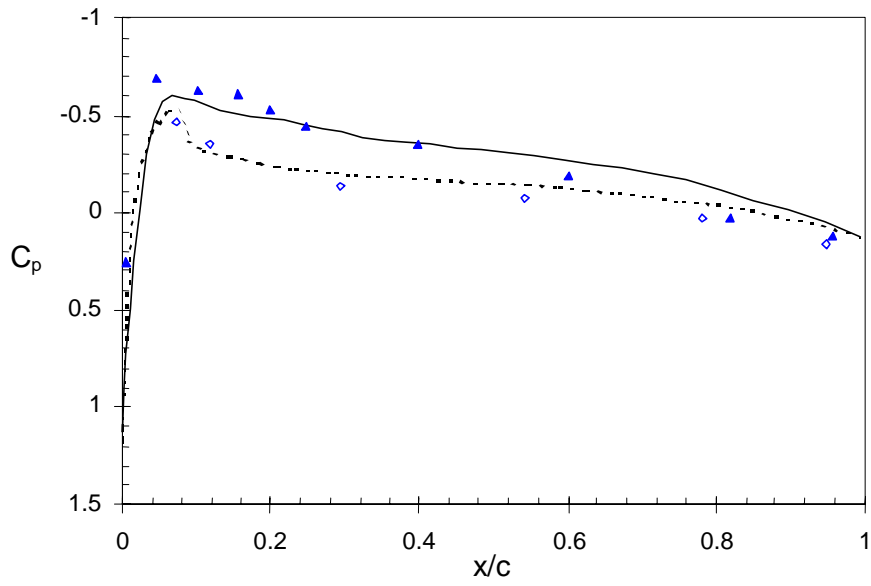
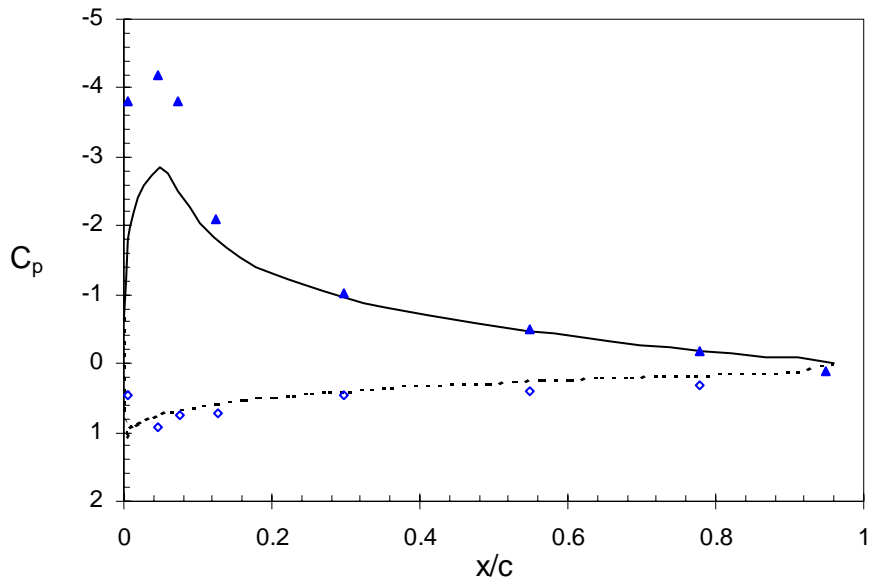


Figure 4.12: Pressure Coefficients for the UH-60A Rotor at $\Psi=180^0$



(a) $r/R=67.5\%$

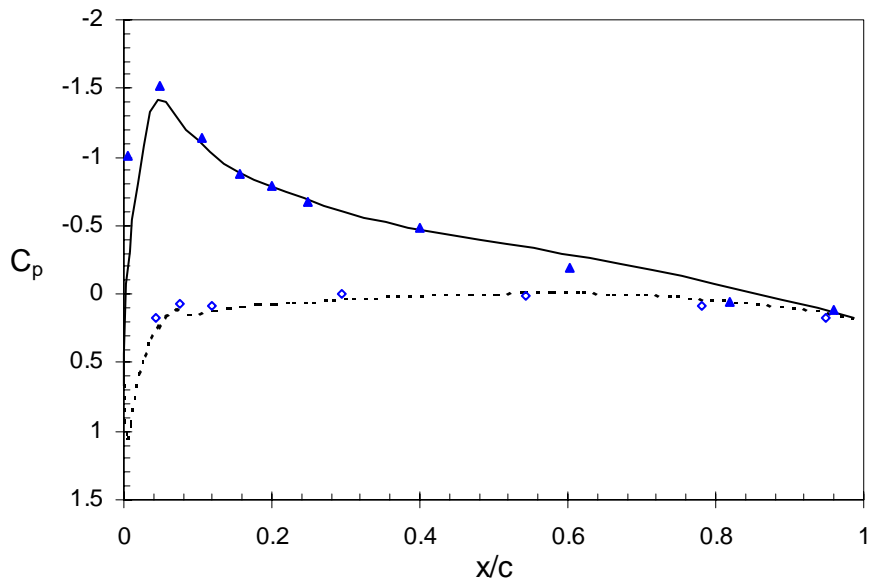
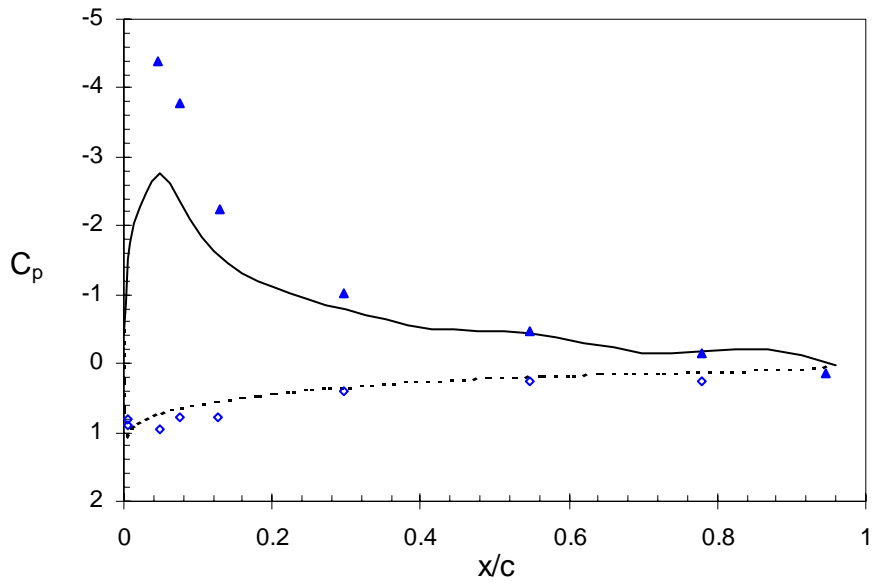


Figure 4.13: Pressure Coefficients for the UH-60A Rotor at $\Psi=210^0$



(a) $r/R=67.5\%$

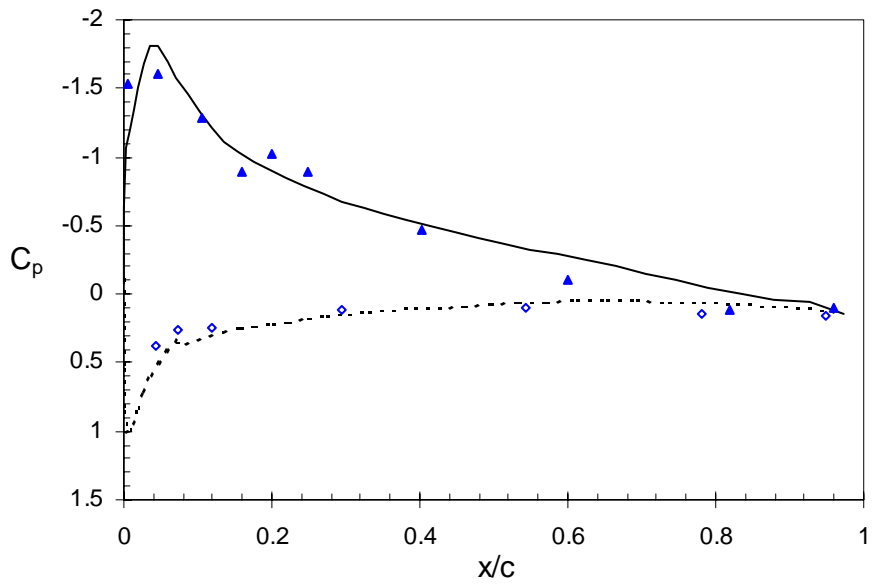
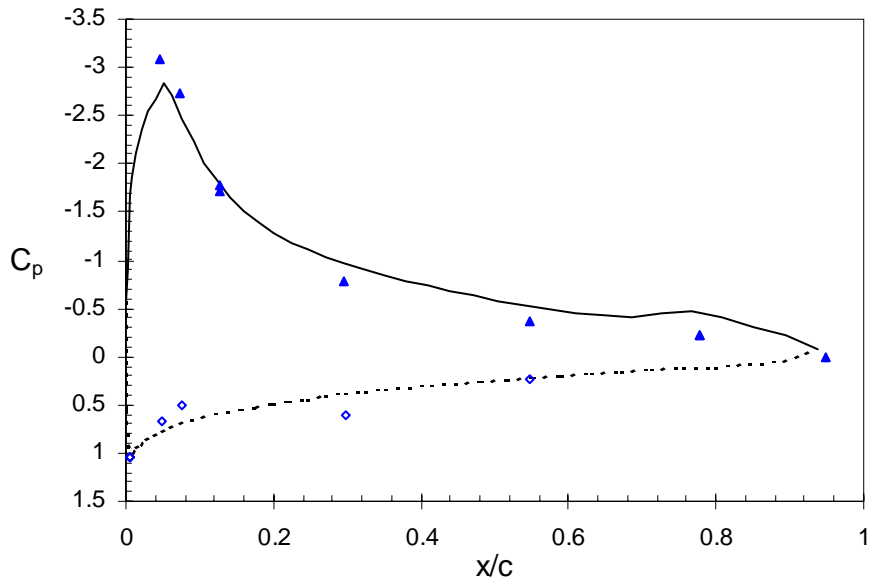


Figure 4.14: Pressure Coefficients for the UH-60A Rotor at $\Psi=240^0$



(a) $r/R=67.5\%$

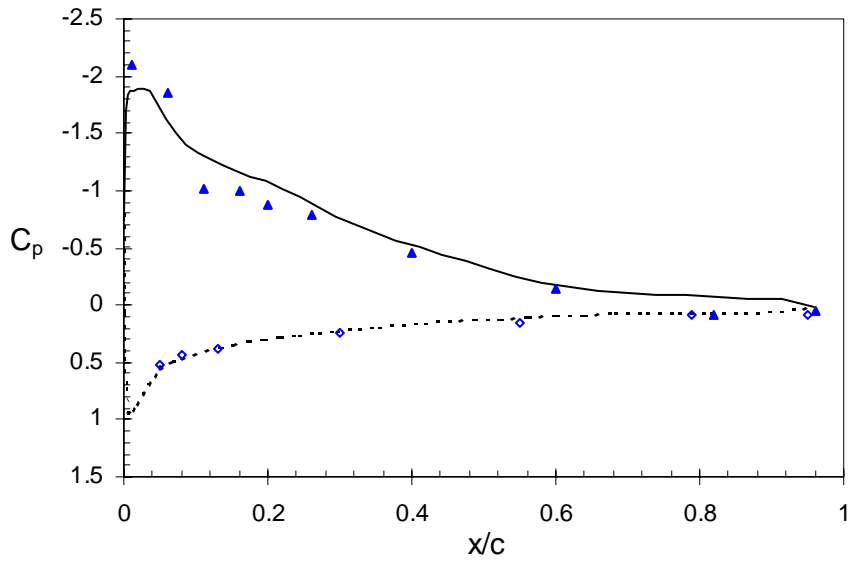


Figure 4.15: Pressure Coefficients for the UH-60A Rotor at $\Psi=270^\circ$

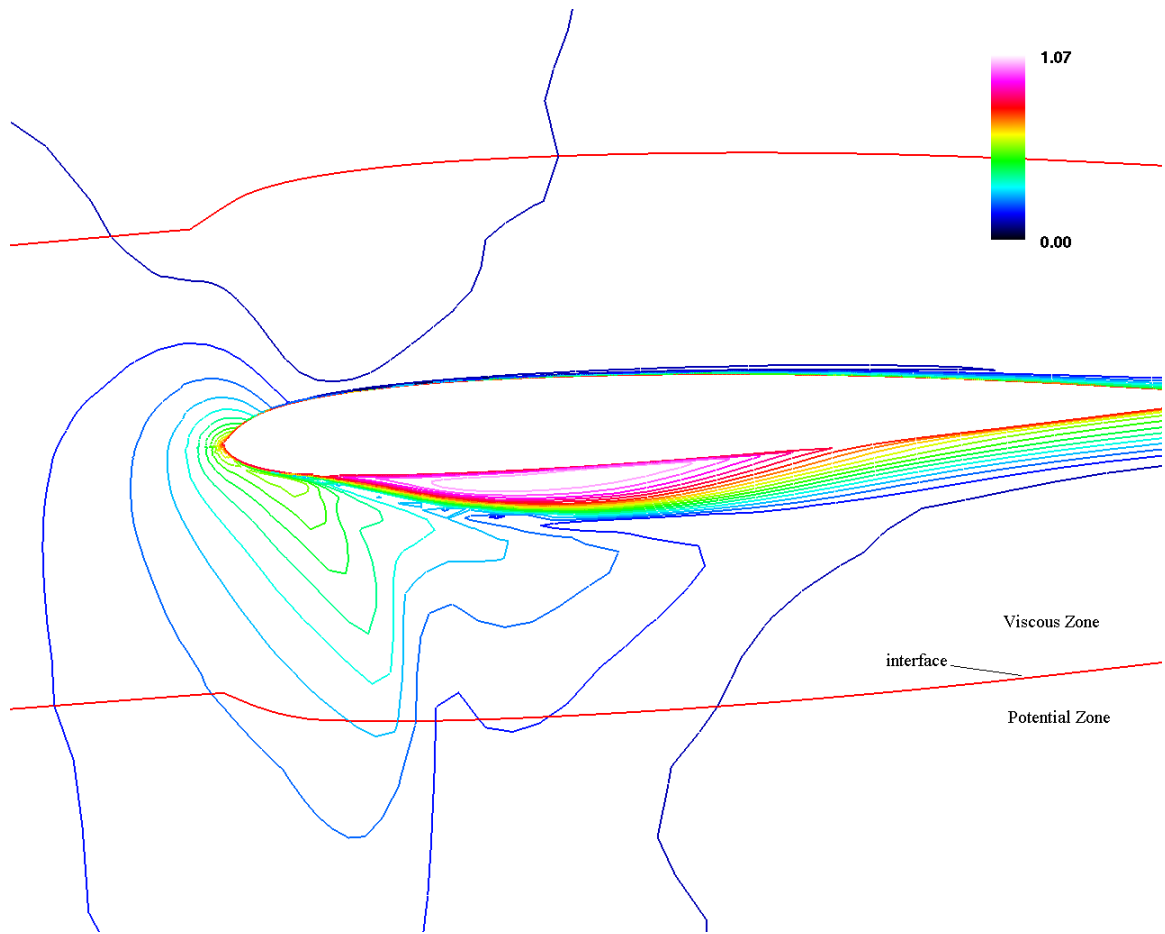
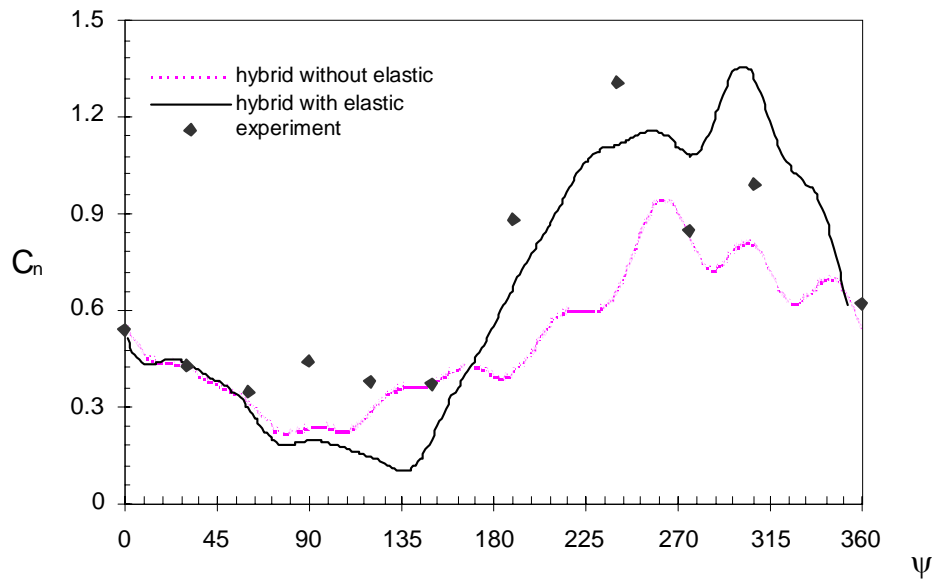


Figure 4.16: Mach Number Contour at $r=96\%R$ (Blade at $\Psi=90^\circ$)



(a) $r/R=67.5\%$

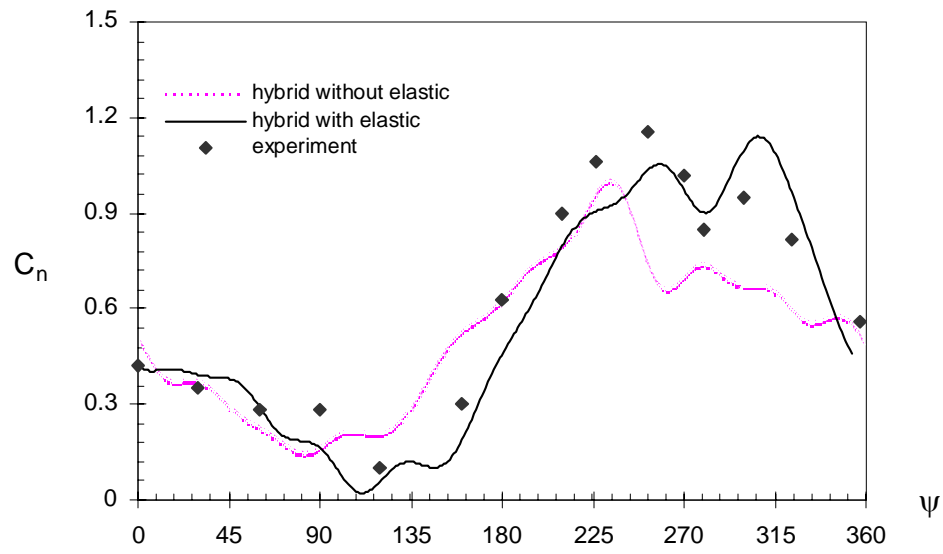


Figure 4.17: Sectional Normal Force Coefficients by the Hybrid Method

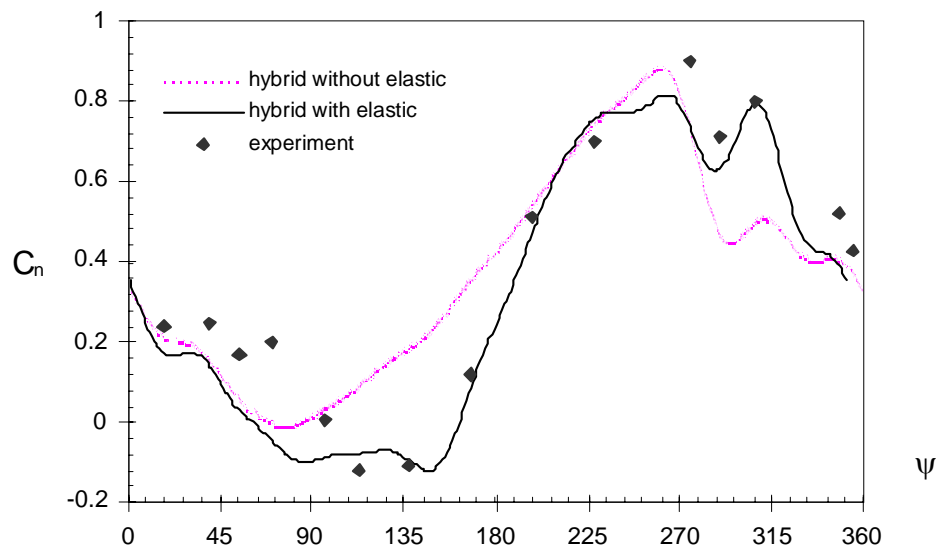
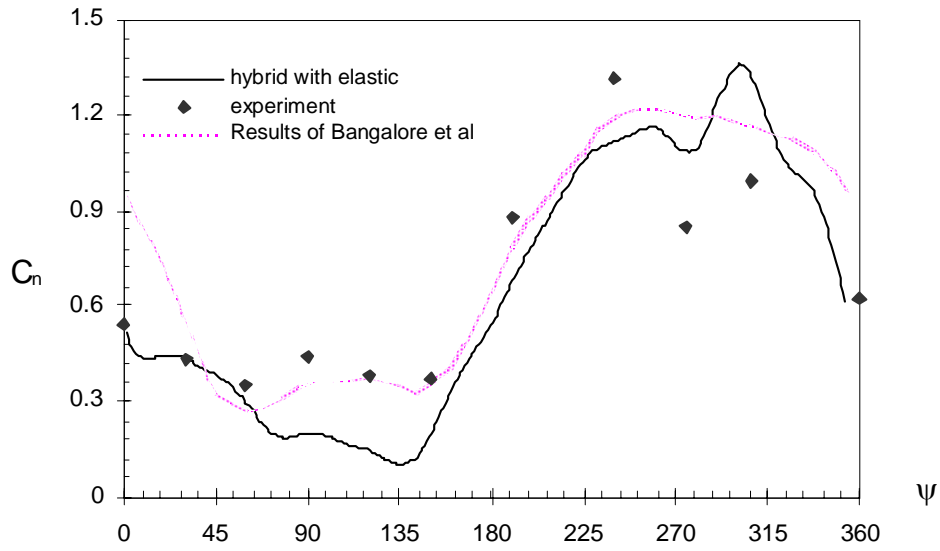


Figure 4.17: Sectional Normal Force Coefficients by the Hybrid Method



(a) $r/R=67.5\%$

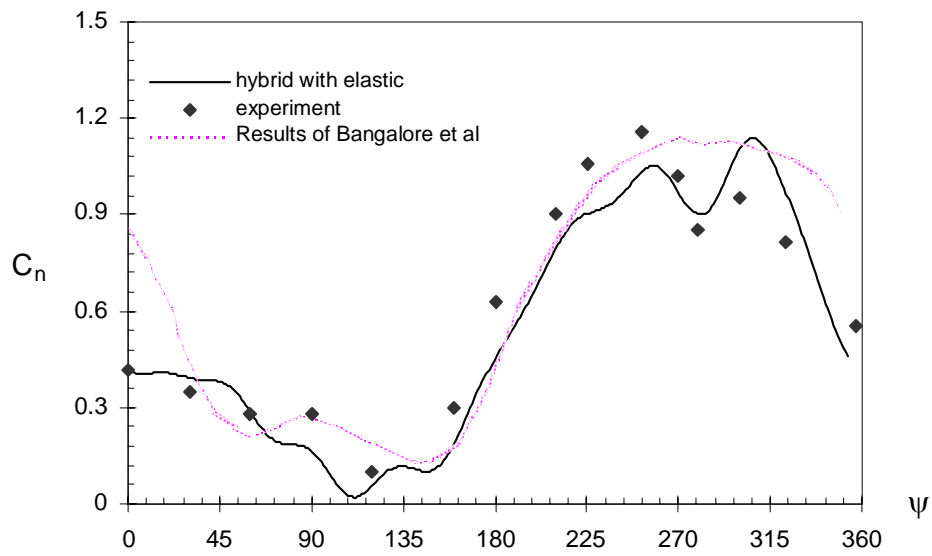
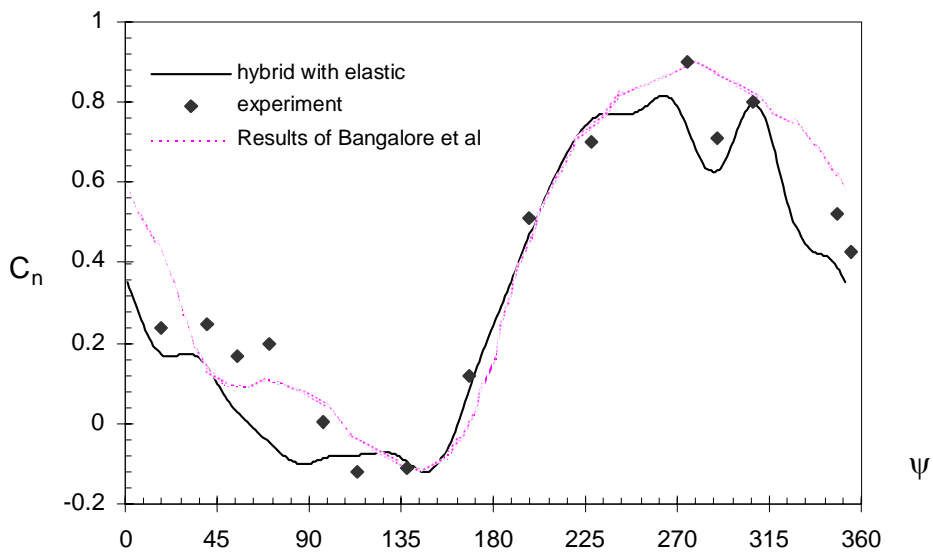
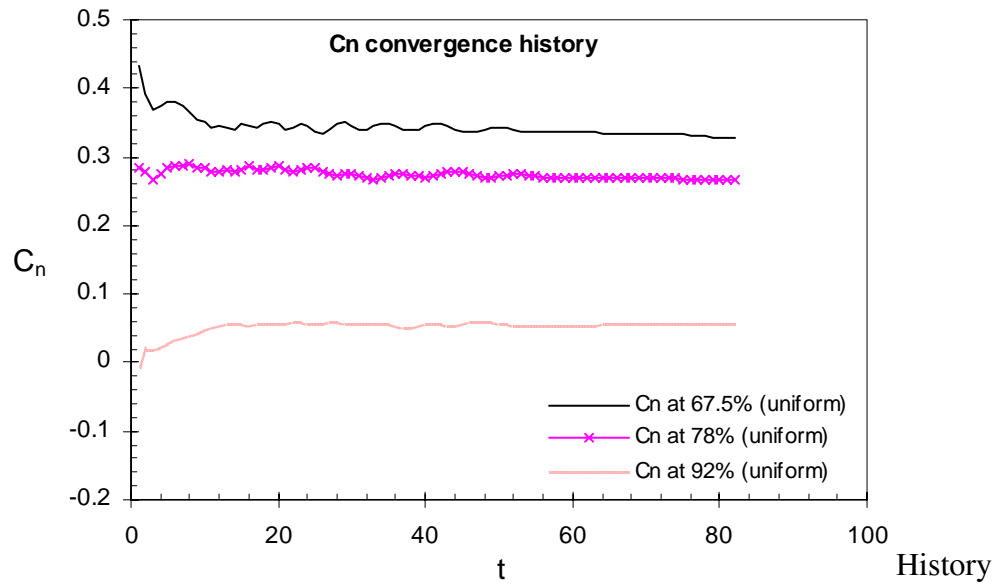
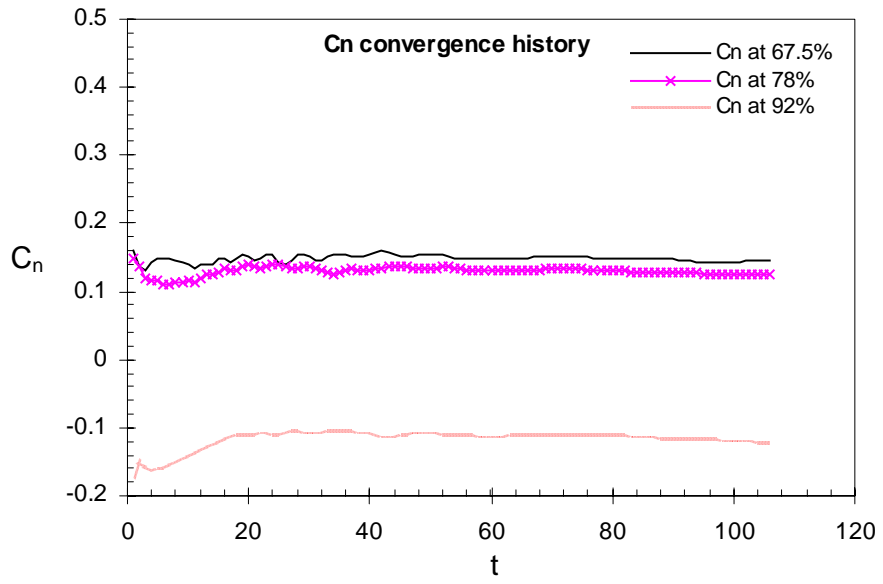


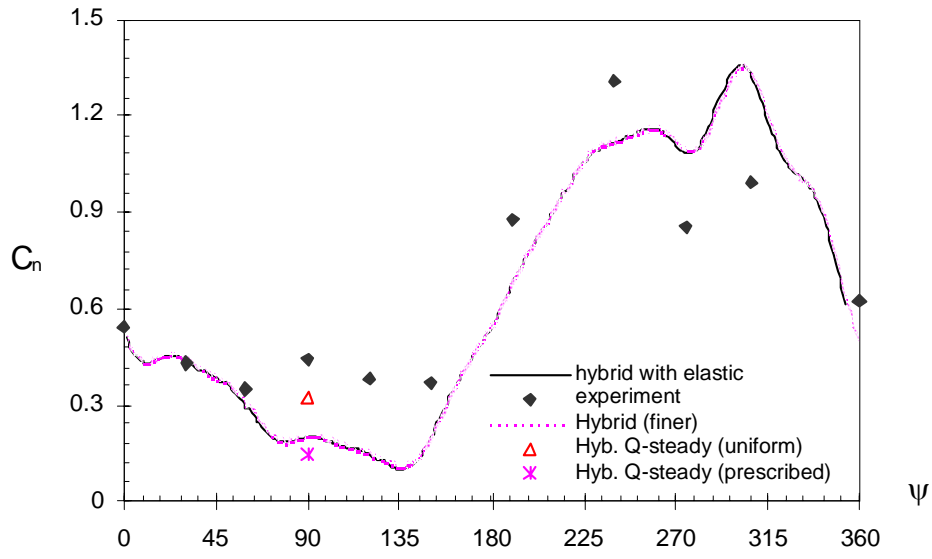
Figure 4.18: Sectional Normal Force Coefficients Compared to Other Computations



(c) $r/R=92\%$

Figure 4.18: Sectional Normal Force Coefficients Compared to Other Computations





(a) $r/R=67.5\%$

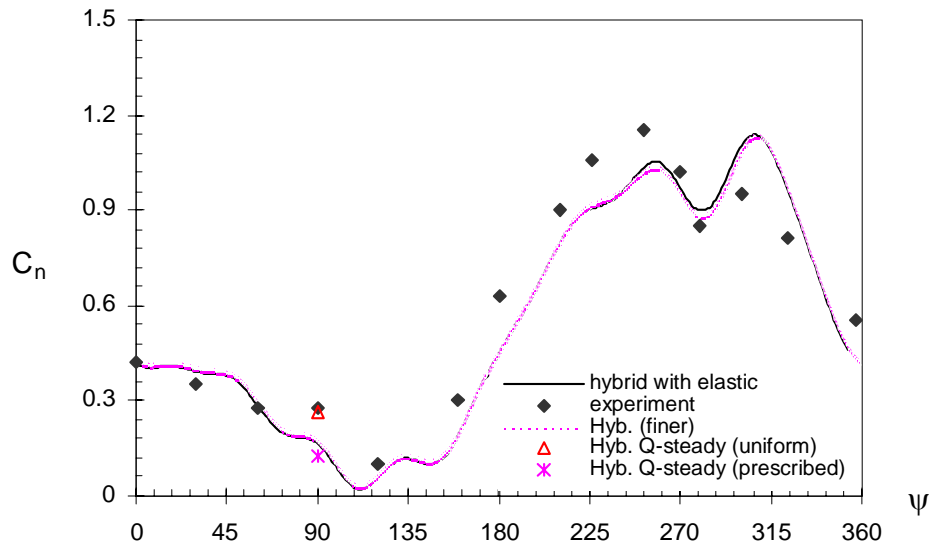
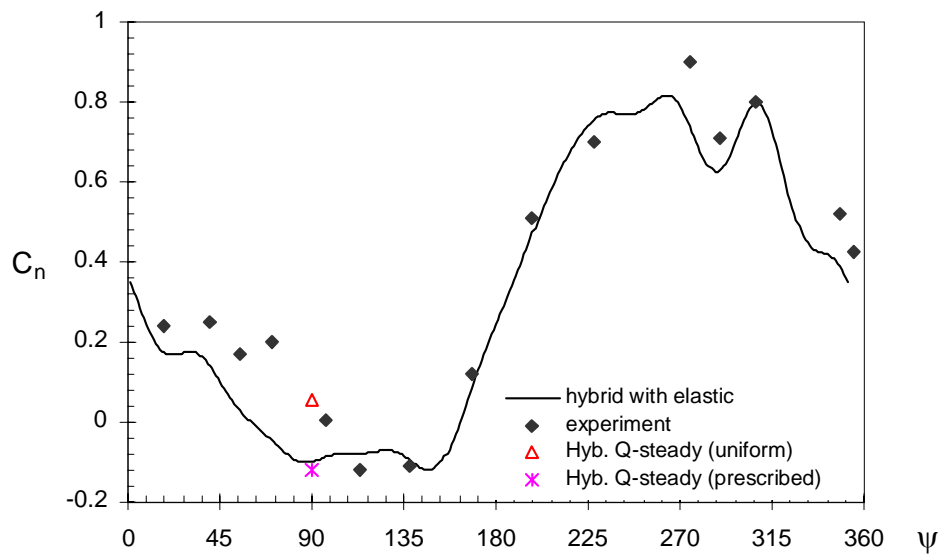


Figure 4.20: Sectional Normal Force Coefficients Compared with the Quasi-steady Solution



(c) $r/R=92\%$

Figure 4.20: Sectional Normal Force Coefficients Compared with the Quasi-steady Solution